Modification of the MARS code for Molten Salt Reactor Applications

Jae Jun Jeong[a]*, Hong Sik Lim[b], Kwi Seok Ha[b], and Yoon Jae Cho[b]
[a]*The School of Mechanical Engineering, Pusan National University, Busan, Korea*
[b]*Korea Atomic Energy Research Institute (KAERI), Daejeon, Korea*
**E-mail: jjjeong@pusan.ac.kr*

Keywords: The MARS code, molten salt reactor, point kinetics model, decay heat model, the GAMMA+ code

1. Introduction

Molten Salt Reactors (MSRs) had been actively developed between the 1950s and 1970s, primarily at Oak Ridge National Laboratory [1]. The key motivations included nuclear-powered aircraft research, enhanced safety, high thermal efficiency, and the potential use of thorium as fuel. MSRs offer several advantages: they operate at high temperatures with low-pressure coolant, reducing meltdown risks, enable continuous fuel recycling, and produce minimal long-lived nuclear waste. However, they faced significant challenges, including material corrosion due to molten salt, immature fuel reprocessing technology, and economic competition from well-established light water reactors.

In recent years, MSRs have regained interest due to their inherent safety, low-carbon energy production, and compatibility with small modular reactor designs. Advances in materials science and fuel reprocessing have addressed previous technical limitations, while the growing demand for sustainable and efficient energy solutions has renewed global interest in MSR technology.

In this study, the thermal-hydraulic system code, MARS, has been modified for MSR applications. The code is based on the consolidated version of the RELAP5/MOD3 and COBRA-TF codes [2]. Since the code was developed for water-cooled reactors, molten slat properties should be implemented first. In addition, nuclear fuel and fission products move along with the carrier molten salt in MSRs. It requires a different approach for reactor kinetics in comparison with those of solid fueled reactors. This paper presents the point kinetics model (PKM) for MSRs, its implementation into the MARS code, and the code verification by code-to-code comparisons.

2. Code modifications for MSR analysis

Various molten salts are being considered for MSR reactors. In this study, the thermal properties of KCl-UCl_3 molten salt were modeled and implemented in the MARS code. Detailed explanations [3] are omitted. This section focuses only on the point kinetics model, decay heat model, and reactivity feedback model

2.1. Point kinetics model

In the MARS code, a point kinetics model with six groups of delayed neutron precursors (DNPs) is adopted [2]. Since the nuclear fuel moves within the reactor cooling system, a significant portion of DNPs is lost outside the reactor. Therefore, β in the conventional PKM should be replaced with β_{eff}:

$$\frac{dN(t)}{dt} = \frac{\rho - \beta_{eff}}{\Lambda} N(t) + \sum_{i=1}^{6} \lambda_i C_i(t) \quad (1)$$

where N: number of neutrons in the reactor core,
ρ: reactivity
β_{eff}: effective fraction of delayed neutrons
Λ: prompt neutron life time
λ_i: decay constant of DNP group i,
C_i: number of DNP group i in the reactor core.

To model the transient behaviors of the DNPs, a transport equation is introduced as follows:

$$\frac{\partial c_i}{\partial t} + \nabla \cdot \left(c_i v_f \right) = \alpha_f f_c \frac{\beta_i}{\Lambda} n(t) - \lambda_i c_i \quad (2)$$

where c_i: density of DNP group i,
v_f: liquid-phase salt velocity,
n: neutron density,
α_f: liquid-phase volume fraction,
f_c: power factor inside the reactor and 0 for outside.

The second term in the left-hand side in Eq. (2) shows that reactor kinetics is directly coupled with thermal hydraulics. The first term in the right-hand side of Eq. (2) is the generation rate by nuclear fission and the second term means radioactive decay. It is noted that $C_i(t)$ in Eq. (1) can be obtained by

$$C_i(t) = \int_{Core} c_i(t) dV ,$$

or

$$C_i(t) = \sum_{j=1}^{NC} c_{i,j}(t) \Delta V_j \quad (3)$$

where NC is the number of computation cells to represent the reactor core and ΔV is the volume of a computation cell. Eqs. (1) through (3) are the governing equations of PKM for an MSR.

When the flow in the reactor coolant system reaches a steady state for a given nuclear power, the distributions of the DNPs inside the reactor core and outside are fixed by Eq. (2) and, then, C_i in Eq. (3) is determined.

Since dN/dt and ρ in Eq. (1) become zero in a steady state, β_{eff} can be obtained as:

$$\beta_{eff} = \frac{\Lambda}{N_o}\sum_{i=1}^{6}\lambda_i C_{io} \tag{4}$$

where C_{io} is C_i at a steady state.

It is noted that, in a steady-state calculation, constant power is given; that is, Eq. (1) is not solved. Instead, null transient advancement for the fluid flow, DNPs, and decay isotopes is carried out to obtain $\beta_{eff,}$ which is used for subsequent transient calculations.

During a transient, the governing equations for fluid flow is solved first in the MARS code. Thereafter, using the new time-step fluid velocity, Eq. (2) is numerically solved, which adopts a first-order finite-difference, upwind, and semi-implicit time scheme. The results are inserted into Eq. (3) to calculate $C_i(t)$. Thereafter, Eq. (1) is solved using the prompt jump approximation as follows:

$$N(t) \approx \frac{\Lambda}{\beta_{eff} - \rho}\sum_{i=1}^{6}\lambda_i C_i(t) \quad . \tag{5}$$

2.2. Decay heat model

A transport equation for decay isotopes can be formulated in the same manner as for the DNPs in Eq. (2):

$$\frac{\partial h_i}{\partial t} + \nabla\cdot\left(h_i v_f\right) = \alpha_f f_c \gamma_i n(t) - \lambda_i h_i \quad . \tag{6}$$

In the MARS code, the ANS 1971/1973 decay heat model is adopted with 11 groups of decay isotopes. Numerical solutions for Eq. (6) are obtained using the same method as for Eq. (2). Then, total reactor power including the fission power and decay heat is

$$Q_{total}(t) = \kappa_e\left(N(t) + \sum_i\sum_k \lambda_i h_{i,k}\Delta V_k\right). \tag{7}$$

The nuclear power in a computational cell k is given by

$$Q_k(t) = \kappa_e\left(f_k N(t) + \sum_i \lambda_i h_{i,k}\Delta V_k\right). \tag{8}$$

The power in Eq. (8) is transferred to all the computational cell of the MARS code at each time step.

2.3. Reactivity feedback model

The reactivity feedback by fuel temperature, fuel density, and reflector temperature was modeled, leading to a total reactivity as:

$$\rho(t) = \rho_{rod} + \rho_{poison} + \alpha_{FT}(T_F - T_{Fo}) + \alpha_{FD}(\rho_F - \rho_{Fo}) + \alpha_{RT}(T_R - T_{Ro}). \tag{9}$$

The control rod reactivity ρ_{rod} is provided as an input data in a tabular form and, the reactivity by poisons ρ_{poison} was not modeled yet.

3. Verification of the code modifications

For the verification of the code modifications, a very simple MSR design was devised. A steady-state and a transient calculation were carried out using the MARS and GAMMA+[4] codes for a comparative analysis.

3.1. A simple MSR design for code verification

The simple MSR consists of a reactor core of 10 MW_t, primary cooling system (PCS), and secondary cooling system. The PCS includes a heat exchanger, a centrifugal pump, an expansion tank filled with helium. The heat generated in the PCS is transferred to the secondary side via the heat exchanger. In the secondary side, a constant flow is provided to cooldown the PCS. The working fluid of the primary and secondary side is the KCl-UCl_3 molten salt.

Basic data of the reactor design is presented in Ref. 3. Fig. 1 shows the MARS nodalization for the simple MSR system. The component 100 in Fig.1 represents the reactor core.

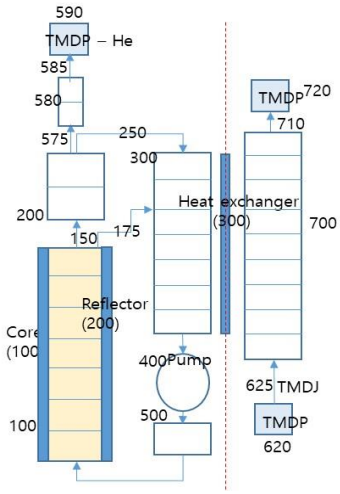

Fig. 1. The MARS nodalization for a conceptual MSR design

3.2. The results of a steady-state calculation

A steady state is obtained by a null transient calculation of 2,000 s with fixed boundary conditions.

Table 1 shows the results of calculations by MARS and GAMMA+. It was found that the molten salt density is greater by ~0.7% in the MARS code. However, the results of the two codes show very good agreement. There are slight difference in the core mass flow rate and, in turn, in $\beta_{eff,}$.

In Table 2, the steady-state distributions for 6 DNP groups at the 7 axial meshes of the reactor core. The maximum relative error between the two codes is 0.17 %. This error is due to the difference of the core flow rate. The distributions of the decay isotopes were also predicted with similar accuracy.

Table 1: Steady state results

Primary side			
	Unit	MARS	GAMMA+
Power	MWt	10.0	10.0
Core inlet temp.	K	868.84	868.61
Core exit temp.	K	908.09	908.52
Mass flow rate	kg/s	514.07	513.45
Beta	-	0.003266	0.003260
Secondary side			
Inlet temp.	K	815.5	815.5
Exit temp.	K	848.37	848.42
Mass flow rate	kg/s	644.33	644.33

Table 2: Steady-state DNP distributions for 6 groups at 7 axial meshes

(a) The MARS results

	1	2	3	4	5	6
1	5.770E+06	4.890E+07	4.438E+08	6.844E+08	3.243E+09	1.501E+09
2	7.772E+06	7.773E+07	6.102E+08	7.607E+08	3.323E+09	1.514E+09
3	8.468E+06	9.487E+07	7.544E+08	8.327E+08	3.401E+09	1.526E+09
4	8.710E+06	1.051E+08	8.794E+08	9.008E+08	3.478E+09	1.539E+09
5	8.794E+06	1.112E+08	9.878E+08	9.651E+08	3.553E+09	1.551E+09
6	8.824E+06	1.148E+08	1.082E+09	1.026E+09	3.627E+09	1.564E+09
7	8.835E+06	1.169E+08	1.163E+09	1.083E+09	3.700E+09	1.576E+09

(b) The GAMMA+ results

	1	2	3	4	5	6
1	5.757E+06	4.875E+07	4.446E+08	6.857E+08	3.247E+09	1.502E+09
2	7.760E+06	7.751E+07	6.098E+08	7.611E+08	3.324E+09	1.514E+09
3	8.457E+06	9.463E+07	7.529E+08	8.323E+08	3.400E+09	1.526E+09
4	8.701E+06	1.048E+08	8.770E+08	8.996E+08	3.475E+09	1.538E+09
5	8.786E+06	1.109E+08	9.846E+08	9.631E+08	3.548E+09	1.549E+09
6	8.815E+06	1.146E+08	1.078E+09	1.023E+09	3.620E+09	1.561E+09
7	8.827E+06	1.167E+08	1.159E+09	1.080E+09	3.690E+09	1.572E+09

3.3. Transient calculation results

The transient behaviors driven by reactivity change in Fig. 2 and the reactor coolant pump trip at 600 s was simulated.

As can be seen in Figs. 2 and 3, the reactor system is exposed only to the reactivity changes until 600 s. Fig. 4 shows the total power vs. time. The two codes present very similar results before the pump trip. This means the reactivity feedback in Eq. (9) and the PKM works well as intended. Also, the two code predicts the molten salt temperatures at the core and the heat exchanger exit very similarly, as shown in Fig. 5.

At 600 s, the pump coast down begins. Fig. 3 shows the GAMMA+ code predicts a rapid flow decrease, reaching an equilibrium earlier. Meanwhile, the MARS code shows a slower and greater decrease. This difference is due to different modeling of the pump inertia and form loss. It again affects the behaviors of the core power and the molten salt temperature in Figs. 4 and 5.

In general, the two codes provide very similar results. The key difference comes from molten salt properties and different modeling of the pump characteristics. It is, however, encouraging that the differences in the results can be explained and easily improved.

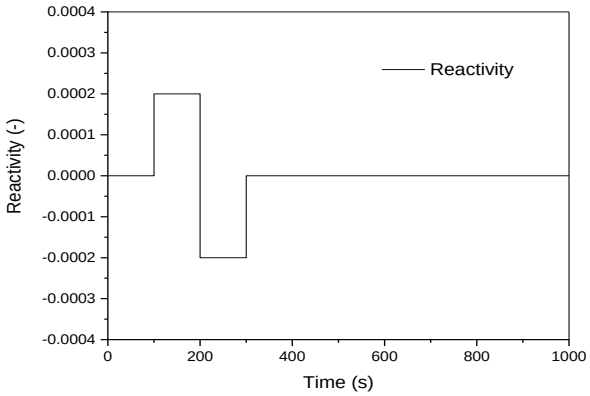

Fig. 2. The reactivity vs. time.

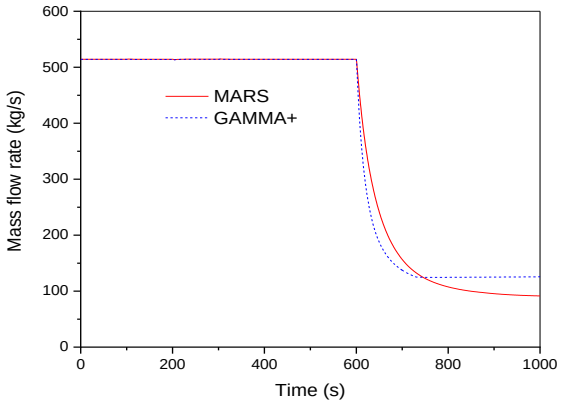

Fig. 3. The core mass flow rate vs. time.

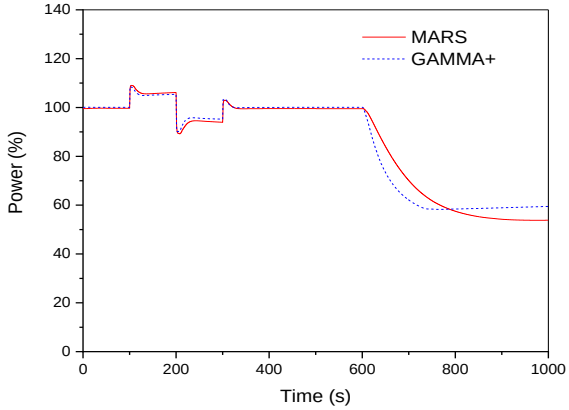

Fig. 4. The total power vs. time.

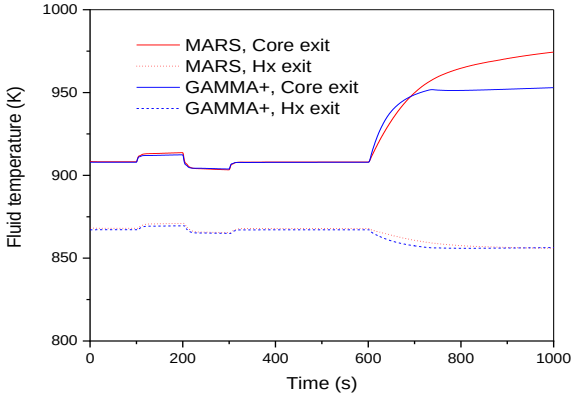

Fig. 5. The molten salt temperature vs. time.

4. Concluding remarks

To extend the applicability of the MARS code to a molten salt reactor, we implemented the molten salt property model for a KCl-UCl_3 first and, then, developed a point kinetics model and decay heat model that can consider the effects of fuel flow in a molten salt reactor. To verify the MARS code modification, steady-state and transient calculations for a simple MSR design were performed using GAMMA+ as well as MARS. The results of code-to-code comparisons were very satisfactory for both the steady state and transient calculations. It was verified that the point kinetics model, decay heat model, and reactivity feedback in the modified MARS code work appropriately.

To make the MARS code a reliable analysis tool for molten salt reactors, systematic validation as well as physical model improvement are needed.

Acknowledgment

This research was supported by the National Research Council of Science & Technology(NST) grant by the Korea government (MSIT) (No. GTL24031-000).

References

[1] D. LeBlanc, Molten salt reactors: A new beginning for an old idea, Nuclear Engineering and Design 240 (2010) 1644–1656.
[2] J.J. Jeong, K.S. Ha, B.D. Chung and W.J. Lee, "Development of A Multi-dimensional Thermal-Hydraulic System Code, MARS 1.3.1," Annals of Nuclear Energy, vol. 26, no. 18, pp. 1611-1642 (1999).
[3] J.J. Jeong, Modification of the MARS code for molten salt reactor analysis, *presented at KAERI*, Feb. 28, 2025.
[4] H.S. Lim, "GAMMA+2.0 Volume II: Theory Manual", KAERI/TR-8662/2021, (July 2021).

Appendix: Comparison of the reactor power behaviors when the material properties and pump models of the MARS and GAMMA+ codes are similarly modified.

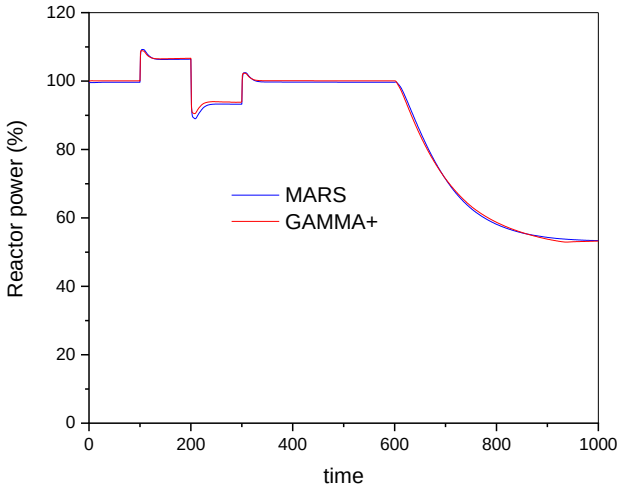

]

Fig. A1. The total reactor power vs. time